

EXPECTED RESULTS FROM CHANNELING RADIATION EXPERIMENTS AT FAST*

J. Hyun, Graduate University for Advanced Studies, Ibaraki, Japan
 D. Broemmelsiek, D. Edstrom, T. Sen†, FNAL, Batavia, IL 60510
 D. Mihalcea, P. Piot, Northern Illinois University, DeKalb, IL 60115
 W. Rush, University of Kansas, Lawrence, KS 66045

Abstract

The photoinjector at the new Fermilab FAST facility will accelerate electron beams to about 50 GeV. After initial beam commissioning, channeling radiation experiments to generate hard X-rays will be performed. In the initial stage, low bunch charge beams will be used to keep the photon count rate low and avoid pile up in the detector. We report here on the optics solutions, the expected channeling spectrum including background from bremsstrahlung and the use of a Compton scatterer during higher bunch charge operation.

INTRODUCTION

Channeling radiation (CR) offers the prospect of a quasi-monochromatic and tunable X-ray source by use of MeV scale electron beams channeling through a thin crystal. Our purpose is to produce high brightness X-rays with low emittance electron beams from a photo-injector and thereby demonstrate a model for a compact X-ray source [1]. By contrast, the most recent experimental channeling results were reported using a thermionic gun in the ELBE linac at the HZDR facility [2].

A new SRF-based photoinjector (formerly ASTA) has been built at Fermilab’s FAST facility and earlier descriptions of the CR experiment can be found in [3, 4]. Fig. 1

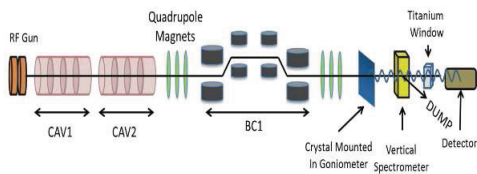


Figure 1: Layout of the experiment. The magnets shown in groups of three are the 1st and 2nd triplets, used for focusing the beam at the crystal.

shows a schematic layout with the rf gun, the two accelerating cavities CAV1, CAV2, the two sets of quadrupole triplets separated by a bunch compressor (BC1), the goniometer (containing the crystal), the vertical dipole magnet for transporting the electrons to the dump and the forward X-ray detector. There are dipole correctors and diagnostic devices including beam current and beam loss monitors and Yag screens for measuring the electron beam size. The crystal for channeling is diamond, with a thickness of 168 μ m

* Fermilab is operated by Fermi Research Alliance LLC under DOE contract No. DE-AC02CH11359

† tsen@fnal.gov

and its surface is cut parallel to the (110) plane. The electron beam has an energy of 5 MeV after the rf gun while the cavities CC1 and CC2 are expected to increase the beam energy roughly by 23 MeV and 16 MeV respectively. Here we will assume that the beam energy at the crystal is 43 MeV. Our operational plan is to start with low bunch charge ~ 20 pC, mainly to enable the bunch to be detected by the BPMs and align the beam in the crystal. However the photon count rate in the forward detector will be high enough to cause pile up. Once the beam is well aligned, the charge will be lowered to ~ 1 pC where the photon rate will be low enough to allow measuring the channeling energy spectrum, without saturation. At high bunch charge ~ 200 pC, the forward detector will be moved off-axis and the X-rays will be Compton scattered off a plastic plate and the spectrum will be recorded on another detector at 90° to the beamline (see Fig.5).

OPTICS SOLUTIONS

The transport of the initial emittance from the photocathode surface to downstream of CAV2 (a distance 8 m from the cathode) was simulated with the tracking program ASTRA [5]. ASTRA includes a cylindrically-symmetric (2+1/2) particle-in-cell space charge algorithm based on a quasi-static approximation. The bunch is modeled as a collection of macroparticles and Poisson’s equation is solved in the beam’s rest frame. The obtained electrostatic fields are Lorentz transformed to the laboratory frame to yield the electromagnetic fields experienced by the macroparticle. In our studies the RF gun parameters (laser spot on cathode, surrounding-solenoid field amplitude, and laser launch phase) and accelerating field of CAV1 were optimized to minimize the transverse beam emittance downstream of CAV2. The laser’s E-field on the cathode was taken to be 40 MV/m consistent with values commonly achieved at FAST. Within the range of charges explored in our simulation ($Q = 1, 20,$ and 200 pC) we find that the transverse emittances remain constant once the beam has been accelerated in CAV2. Simulations in the following beamline sections can consequently be done with single-particle-dynamics tracking codes such as ELEGANT or SAD.

An important requirement on the optics is that the beam divergence at the crystal should be less than the critical angle for channeling. At 43 MeV, this critical angle is 1.1 mrad. A small divergence requires that there be a waist in the optics ($\alpha_x = 0 = \alpha_y$) at the crystal. The smallest beam size at the crystal, compatible with the available emittance and divergence requirement, will yield a higher spectral

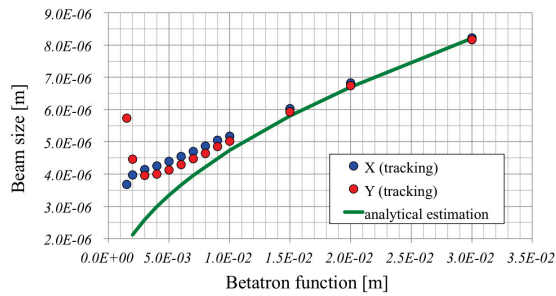


Figure 2: Beam size at the crystal as a function of the beta function at the crystal. The dots show the beam size as found by tracking with SAD while the green curve shows the value $\sigma = \sqrt{\beta\epsilon}$. Below $\beta = 3\text{mm}$, the vertical beam size is dominated by the chromatic aberrations.

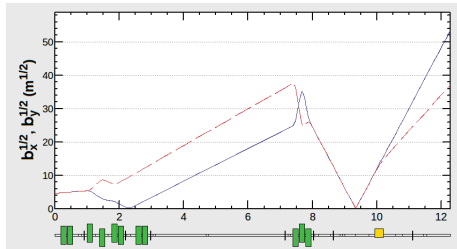


Figure 3: $\sqrt{\beta}$ along the beam line. The waist is at the location of the crystal. Upstream of the crystal, the beta functions reach maximum values in the second triplet. The beam dump is at the end of this beamline.

Table 1: Bunch charge, the expected normalized emittance ϵ_N , minimum beam size at the crystal σ_{cr} , rms divergence at the crystal σ'_{cr} and maximum rms beam sizes in the second triplet.

Charge [pC]	ϵ_N [mm-mrad]	σ_{cr} [μm]	σ'_{cr} [mrad]	$\sigma_x^{max}, \sigma_y^{max}$ [mm]
1	0.023	1.3	0.3	(0.54, 0.6)
20	0.19	4	0.86	(1.5, 1.7)
200	0.52	9.8	0.9	(1.7, 2.0)

brilliance and lower background from bremsstrahlung. The maximum beam size in the final quadrupole triplet should be small enough to allow sufficient physical aperture. Finally, optics solutions must be available over the entire operating range of bunch charges and emittances. The optics solutions presented here were done with the program SAD [6]. Fig. 2 shows the beam size at the crystal as a function of the beta function at the crystal for a bunch charge of 20 pC. The rms momentum spread is 0.1 %. The dots show the beam size obtained from tracking while the curve shows the value $\sqrt{\beta\epsilon}$, ϵ is the un-normalized emittance. The minimum vertical beam size is reached at $\beta_y = 3\text{mm}$. Below this value, chromatic aberrations due to the large β values in the final triplet start to dominate and increase the beam size. Fig. 3 shows the $\sqrt{\beta_x}, \sqrt{\beta_y}$ values along the beamline. Table 1 shows the minimum beam sizes obtainable at the crystal for

three values of the initial bunch charge. The beam pipe radius in the quadrupoles is 27 mm, so there is sufficient aperture for the beam ($> 13\sigma$) in all solutions. Low divergence solutions ($\sigma'_{cr}=0.1\text{mrad}$ for all charges) have also been generated. These have the advantage of higher photon yields (and larger signal above background) but at the expense of spectral brilliance.

BREMSSTRAHLUNG BACKGROUND

The largest source of background to the channeling radiation is expected to be bremsstrahlung (BS) from the crystal. Both BS and CR will be emitted in the forward direction and enter the forward detector acceptance. Dark current from the rf gun may also create some background, but it is likely that this dark current will be bent away from the crystal by the bunch compressor chicane upstream of the crystal. The BS cross-section for number of photons into an energy range dE_X and solid angle $d\Omega$ scales with electron beam's Lorentz factor γ and the photon energy E_X as $d^2N_{ph}/dE_X d\Omega \sim \gamma^2/E_X$. The BS background expected in this experiment have been calculated with the program Geant4 [7], see Fig. 4. The spectrum is broad-band ranging up to tens of MeV with an electron beam of 43 MeV. The angular distribution is also wider than CR, with an rms spread of 49 mrad compared to 12 mrad for CR. Since the detector acceptance will be of the order of a few mrad, the BS distribution over the detector plate is expected to be uniform.

CHANNELING SPECTRUM

The CR spectrum for beam energies $< 100\text{MeV}$ can be calculated by solving Schrodinger's equation for electrons propagating in the transverse potential of the crystal atoms. If the electron is localized in a bound state of this potential, it can emit radiation at discrete frequencies in transitions between these bound states. Otherwise, if the electron transverse energy is high enough to be in a free quantum state, then any radiation it emits would form a continuous spectrum and would not be channeling radiation. Many processes such as multiple Coulomb scattering or thermal scattering can increase the transverse energy and lead to dechanneling. The CR energy emitted in transitions between two bound states scales approximately with the electron's energy as $E_X \sim \gamma^{5/3}$ while the energy spread scales as $\Delta E_X/E_X \sim \gamma^2$. A complete calculation of the expected photon yield at FAST and successful comparisons with the results obtained at ELBE was reported in [8]. There it was shown that the process of rechanneling in which an electron from a free state is scattered back into a bound state has an important impact on the channeling yield. This mix of dechanneling and rechanneling was modeled by introducing a free state index n_f such that electrons entering state n_f and higher do not rechannel back into a bound state while all states below n_f can via rechanneling contribute to the channeling photon yield. The value of n_f depends on the beam energy, crystal thickness etc and we treat it as a free parameter. Low values of n_f

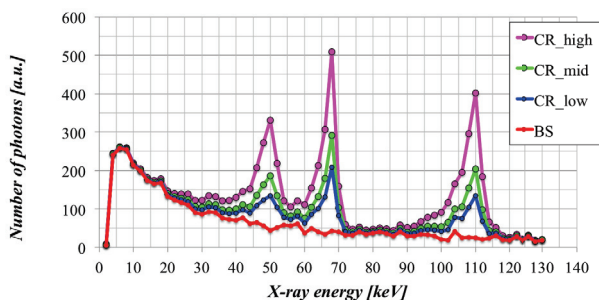


Figure 4: Bremsstrahlung spectrum (in red) and the total spectrum (BS + CR) for different estimates of the CR photon number.

would reduce the rechanneling and result in a low photon yield.

Fig. 4 shows the CR yield for three values of n_f , labeled low, mid and high, superimposed on the bremsstrahlung spectrum. The bunch charge was 20 pC, the beam energy 43 MeV and the beam divergence was set to 0.1 mrad. We assumed here that the detector acceptance is 2 mrad in each transverse plane. There are three distinct CR peaks at 51 keV (from the $3 \rightarrow 2$ transition), at 67.5 keV (from the $2 \rightarrow 1$ transition) and at 110 keV (from the $1 \rightarrow 0$ transition). The linewidth for each line is about 10 %. In this calculation, the signal to background ratio for the 110 keV line for example, ranges from 4 (low) to 7 (mid) to 15 (high). These ratios will change depending on the beam divergence at the crystal but should be independent of the charge.

COMPTON SPECTROMETER

Even at a bunch charge of 20 pC, the photon rate in the forward detector is expected to be high enough to cause pulse pileup. We have devised three scenarios to deal with this issue. One will be to use low bunch charge, as low as 1pC, to reduce the photon rate. However, diagnostics and especially the BPMs, are not sensitive to bunch charges below 20 pC, so this will only be done after the beamline has been tuned and aligned with higher bunch charge. At moderate bunch charge, brass collimators with openings of either 0.4 mm or 1 mm will be attached to the forward detector to reduce the detector acceptance. At the highest bunch charge (~200 pC) the forward detector which is mounted on a movable stage, will be moved off-axis and a Compton scatterer (a square 5 cm x 5 cm plate of polycarbonate, 2 mm thick) will be inserted in the beamline about 79 cm from the diamond window. Fig. 5 shows a sketch of this configuration. A second detector at 90° will be used to detect the Compton scattered X-rays. The Compton scatterer will change the photon energy by a few % and the photon flux by orders of magnitude. At 90°, the 67.5 keV line is expected to shift down to 60 keV. The Klein-Nishina expression for the differential cross-section for Compton scattering shows that the photon flux has a minimum at 90°. Fig. 6 shows a Geant4 calculation of the expected photon energy spectrum with a

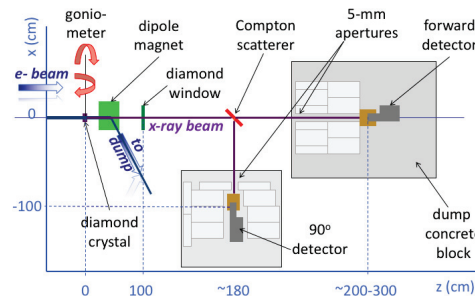


Figure 5: Schematic of the layout showing the Compton scatterer, the 2nd detector at 90° to the beamline and shielding around the 1st detector. Note that the figure is not to scale.

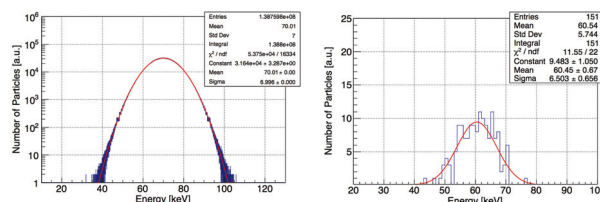


Figure 6: Energy distribution of 67.5 keV photons passing through a 2 mm thick PVC plate. Incident number of photons= 10^9 . Left: Forward photons, Right: Photons scattered at 90°.

2 mm thick PVC plate. Relative to the forward photon number, the photon number at 90° is reduced by about six orders of magnitude. This will be sufficient to allow a measurement of the X-ray spectrum without pileup issues.

X-RAY DETECTOR CALIBRATION

The forward X-ray detector (Amptek CdTe X-123, area $3 \times 3 \text{ mm}^2$, nominal thickness 1 mm) has been calibrated with Co57 spectra which emits lines at 14.4 keV and 122 keV. Several settings in the digital processor of the detector were optimized. The thresholds of the slow channel (which measures the pulse height), the fast channel (which serves as a pileup rejection) and the peaking time which is the time taken by the slow channel to measure the pulse were optimized for energy resolution and count rate. The detector efficiency over the energy range 10-150 keV has been calculated from the measured Co57 spectrum and will be used in correcting the measured CR spectrum. Finally, the phenomenon of “hole-tailing” in CdTe which results in long low energy tails above 100 keV has been accounted for by using the full width at (1/10)th the maximum (FW0.1M) as the width of a spectrum peak. This leads to a consistent photon count for all peaking times.

REFERENCES

- [1] C. Brau et al, *Synch. Rad. News*, **25**, 20 (2012)
- [2] W. Wagner et al, *Nucl. Inst. & Meth.*, **B 269**, 327 (2008)
- [3] P. Piot et al, *AIP Conf. Proc.*, **1507**, 734 (2012)

- [4] D. Mihalcea et al, Proc. IPAC15, 95 (2015)
- [5] K. Flöttmann, Astra user manual, available from DESY, Hamburg.
- [6] <http://acc-physics.kek.jp/SAD/>
- [7] <https://geant4.web.cern.ch/geant4/>
- [8] T. Sen and C. Lynn, Int. J. Mod. Phys. A, **29**, 1450179 (2014)